Target coverage and selectivity in field steering brain stimulation

Ruben Cubo[1], Mattias Åström[2], and Alexander Medvedev[1]

***Abstract*— Deep Brain Stimulation (DBS) is an established treatment in Parkinson's Disease. The target area is defined based on the state and brain anatomy of the patient. The stimulation delivered via state-of-the-art DBS leads that are currently in clinical use is difficult to individualize to the patient particularities. Furthermore, the electric field generated by such a lead has a limited selectivity, resulting in stimulation of areas adjacent to the target and thus causing undesirable side effects. The goal of this study is, using actual clinical data, to compare *in silico* the stimulation performance of a symmetrical generic lead to a more versatile and adaptable one allowing, in particular, for asymmetric stimulation. The fraction of the volume of activated tissue in the target area and the fraction of the stimulation field that spreads beyond it are computed for a clinical data set of patients in order to quantify the lead performance. The obtained results suggest that using more versatile DBS leads might reduce the stimulation area beyond the target and thus lessen side effects for the same achieved therapeutical effect.**

I. INTRODUCTION

Deep Brain Stimulation (DBS) has been used as a last resort therapy to alleviate the symptoms of various neurological diseases, such as Parkinson's Disease (PD) [1], epilepsy [2] and dystonia [3]. In addition, the interest in this therapy has spread to the treatment of psychiatric disorders such as obsessive-compulsive disorder [4] and schizophrenia [5]. The principle of DBS is in delivering mild electrical pulses via a chronically implanted lead, whose active contacts are in the subcortical area, where a stimulation target is defined.

Compared to other methods, such as ablation and lobotomy, DBS is reversible to a large extent and more flexible [6]. However, the physiological mechanism of DBS and its long-term effects on the brain still remain unknown, and the therapeutical outcome is difficult to predict. Furthermore, because of uncertainties in the position of the leads [7] or improperly tuned stimulation settings, the stimulated volume might go beyond the target causing undesirable side effects [8], [9]. Shaping the stimuli so that the stimulated volume covers the intended target and does not spill outside of it is thus vital for maximization of the therapeutical benefits and minimization of the side effects.

Currently used lead designs, mostly from Medtronics, were originally adapted from cardiac pacing technology and have not evolved much since then. Meanwhile, the insights into neurostimulation and field steering obtained in recent years through Finite Element Method (FEM) based multiphysics simulation and neuron models, along with the exponential improvement of computational capabilities, open up for more sophisticated and individualized solutions. To address the shortcomings of the widely used design, novel leads have been developed by companies such as 3Win (Belgium), Sapiens (The Netherlands) and Aleva (Switzerland) that could be configured in more versatile spacial settings, taking advantage of field steering techniques to tune the stimuli [10], [11].

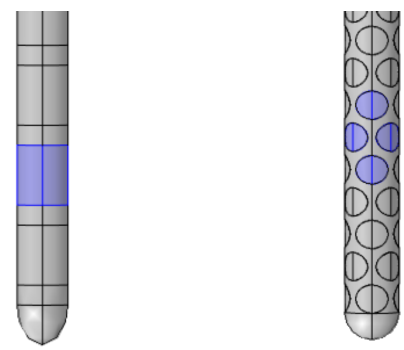

Fig. 1. Design of a conventional (left) and a field steering (right) lead. Active contacts configurations used in simulation are rendred in blue.

While a conventional state-of-the-art lead delivers a radially symmetric stimulation over the whole cylindrical contact, a field steering one is capable of asymmetrical stimulation that can be tailored to the target area anatomy, as seen in the contacts geometry of the leads in Fig. 1.

In this study, a quantitative performance analysis of a basic field steering configuration compared to a conventional one is performed by means of a multiphysics simulation model with clinical stimulation settings, first for a patient and afterwards for a clinical data set of different leads.

II. MODELS AND METHODS

A. DBS Model

The simulation model used in this study consists of three parts: the lead, the brain bulk tissue, and the encapsulation layer. Two lead designs are considered: a widely used state-of-the-art lead and a field steering lead. The former has cylindrical contacts with a height of 1.5 mm and a separation between contacts of 0.5 mm. The latter has elliptical contacts. To facilitate field steering, the rows are rotated 45 degrees to each other with respect to the lead axis, as shown in Fig. 1 (right). Both leads have a diameter of 1.27 mm.

[1]R. Cubo and A. Medvedev are with Department of Information Technology, Uppsala University, 751 05 Uppsala, Sweden

[2]M. Åström is with the Department of Biomedical Engineering, Linköping University, 581 83 Linköping, Sweden

*RC and AM were partially supported by funding from the European Research Council, Advanced Grant 247035 (ERC SysTEAM)

The bulk tissue is represented as a cube with a side of 0.4 m centered on the tip of the lead that is grounded on the outer surfaces. Although the brain tissue is in reality heterogeneous and anisotropic, these effects are not considered here. Thus, the bulk tissue is modeled as a homogeneous medium with a conductivity of 0.1 S/m [13].

An encapsulation layer is formed around a lead implanted in the brain. Its thickness and conductivity are still open to debate and might be patient specific. Following [8], a 0.5 mm thick layer with a conductivity of 0.18 S/m is considered.

The stimulation is modeled as a boundary condition at the active contacts surface while the non-active contacts are left floating. The electric potential and field distributions in the tissue are computed by solving the equation of steady currents in the tissue:

$$\nabla \cdot (\sigma \nabla u) = 0, \tag{1}$$

where u is the potential, σ the electric conductivity and ∇ is the vector differential operator.

The model has been implemented in COMSOL 4.3b (Comsol AB, Sweden), with approximately 9,000,000 and 2,800,000 degrees of freedom for the field steering and the state-of-the-art leads, respectively. The solutions obtained by FEM were then equidistantly gridded on a 70x70x60 grid centered at the lead tip and expanding 16 mm in the axes perpendicular to the lead and 20 mm in the lead axis, in order to be exported for further processing.

Clinical data from 82 implanted Medtronics 3389 leads, namely the position of the most distal contact, the lead vector (defining the lead orientation), and the corresponding stimuli potentials are used for the lead and the stimulation settings in the model. Since the field shapes are different, to enable a fair comparison between the leads given a certain level, the computed electric field isosurfaces are adjusted to have the same maximum radius for both lead types. Diamond-4 configuration depicted in Fig. 1 is utilized in this study as the most selective one for field steering [15].

B. *Quantification of activated volumes*

Traditionally, activated volumes are quantified by using either axon models under the methodology given by McNeal [17] or functions that approximate the activated volume disregarding the anatomy of the neurons, such as Rattay's activation function [16], [18] or the electric field [14]. While using axon models yields accurate results, it is computationally expensive. On the other hand, based on the calculation of the second spatial derivative, making use of Rattay's activation function might result in numerical issues, particularly near the lead and in the interface between the encapsulation layer and brain tissue. Thus, this study will use the electric field to account for neuronal activation since it is straightforward to compute and is not sensitive to the smoothness of the model solutions as the second derivative. The activated neurons are distinguished from the rest by applying a threshold value for the electric field. For illustration, the threshold is here set to 200 V/m.

To place the previously computed electric field at the proper position, conventional translation-rotation algebra is utilized. In particular, axis-angle formalism is applied defining a rotation vector and an angle given by

$$\mathbf{v}_{\text{rot}} = \mathbf{v}_{\text{lead}} \times \mathbf{v}_{\text{data}},$$

$$\theta = \arccos(\mathbf{v}_{\text{lead}} \cdot \mathbf{v}_{\text{data}}),$$

where $\mathbf{v}_{\text{rot}}$ is the axis of rotation, $\mathbf{v}_{\text{lead}}$ is the initial lead direction that is assumed to be the Z axis, $\mathbf{v}_{\text{data}}$ is the lead vector from the lead data, and θ is the rotation angle. This is then converted into a rotation matrix. In addition, since the field distribution asymmetry is of particular interest, the lead is rotated with respect to its longitudinal axis before performing other operations. Assuming that the lead is centered properly, the set of operations is given by

$$\mathbf{E}_{\text{eval}} = R_{\text{rot}} R_{\text{z}} \mathbf{E} + \mathbf{x}_{\text{lead}},$$

where $\mathbf{E}$ and $\mathbf{E}_{\text{eval}}$ are the original and positioned electric field vectors respectively, R_{rot} is the rotation matrix described above, R_z is a rotation matrix with respect to the Z axis, and $\mathbf{x}_{\text{lead}}$ is the lead position. These operations are implemented in MATLAB 2013b (The MathWorks, USA).

Once the field is properly positioned and filtered, intersection volumes can be computed. Two of them are of particular interest: the activated volume of the target area and the activated volume outside the target area. However, the lead should be considered when computing the volumes. Since the lead geometry is simple and its properties are known, it can be easily subtracted from the evaluated volumes. The topology of the target area is taken from an atlas of potential regions for therapeutical stimulation and can be assumed to be convex, to facilitate checking whether or not the electric field distribution points are inside the convex hull of the target area*.

To illustrate the activation in a more intuitive manner, instead of providing the absolute volume values, they are calculated as fractions of the total volumes considered: the target area for the activated volume and the total electric field volume for the overspilled volume.

The ultimate field steering objective is thus to achieve an activation fraction close to 100%, while keeping the overspill fraction as low as possible.

III. RESULTS

A. *Single patient evaluation*

An overview of the isosurfaces such as the one in Fig. 2 suggests that the stimuli applied to the patients should cover the entire area. However, the stimuli seem to also reach a large surrounding volume, so the overspilled amount should be quite significant as well.

To illustrate the effects of the asymmetrical configuration with respect to the conventional one, the data of one patient are analyzed in detail. Table I summarizes some of the available data, such as the active contact (assuming that

*Function created by John D'Errico (MATLAB Exchange) is used.

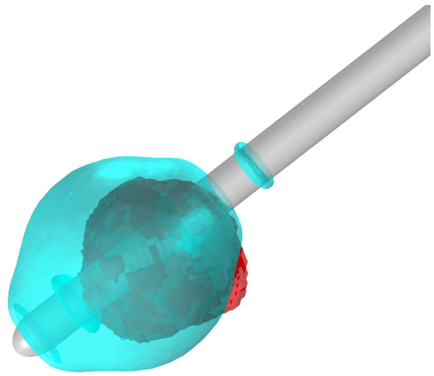

Fig. 2. Electric field distribution sample (cyan) surrounding the target area (red).

contact 0 is the most distal one) and the stimuli amplitude given, which will be the same as the one used for the state-of-the-art lead in the study. In Fig. 3, a polar plot specifying the activation and overspilled percentages is as well provided.

While the conventional lead produces as expected the same field for any rotation angle, some variations can be seen in the field steering one due to the asymmetry of the active contacts. In the latter case, the activated volume varies between its maximum and a significantly lower value depending on the rotation with respect to the lead. The situation with the overspilled volume is similar, although it does seem to be less significant. Nevertheless, for angles where the activation volume is maximal for the field steering lead in Diamond-4 configuration, the overspill is approximately 22% lower than for the other lead for the same patient.

TABLE I
STIMULATION DATA AND RESULTS

Active contact (from Medtronics data)	1
Stimulus amplitude (from Medtronics data)	2.8 V
Stimulus amplitude (field steering)	3.4 V
Maximum activation (conventional)	81.8 %
Maximum activation (field steering)	83.7 %
Overspill (conventional)	78.2 %
Minimum overspill (field steering)	61.0 %

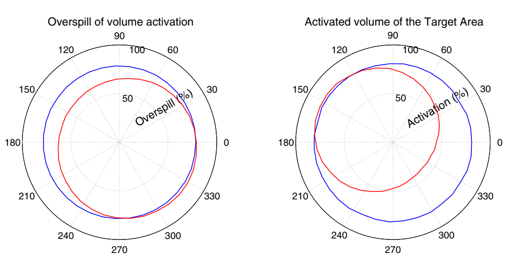

Fig. 3. Evaluation of the activated and overspilled volumes with respect to the rotation angle of the conventional (blue) and the field steering (red) leads.

B. Evaluation over a clinical data set

In order to perform an informative study over a clinical data set from different patients, a statistical evaluation is proposed. With the same procedure as above, the minimum overspilled activation and the maximum target area activation are evaluated for each lead. The results are then compiled for the whole set and plotted in a histogram.

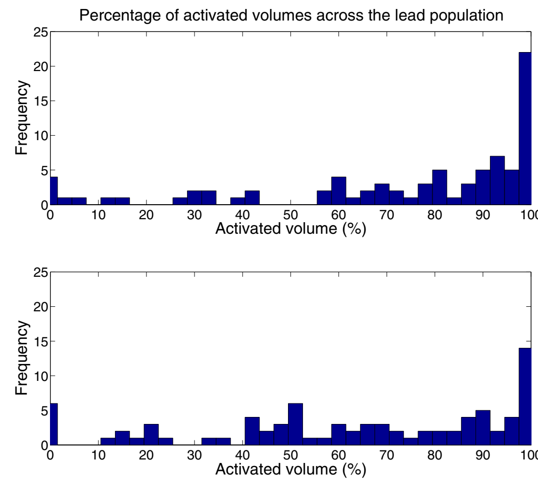

Fig. 4. Activated volumes across the clinical data for the conventional lead (top) and the field steering lead (bottom)

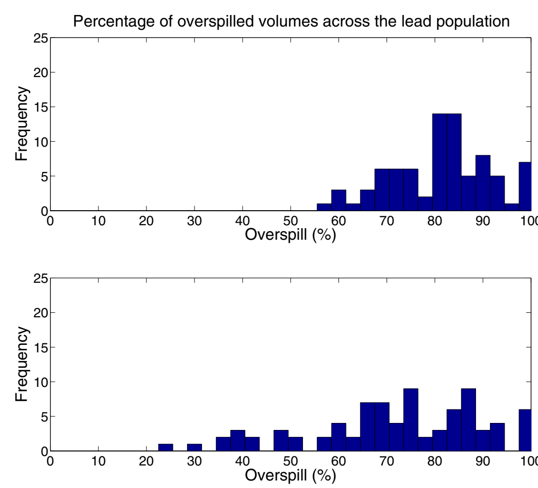

Fig. 5. Overspilled volumes across the clinical data for the conventional (top) and the field steering lead (bottom)

Activation of the target area is achieved for most of the lead settings for both leads, as seen from Fig. 4. However, when it comes to the overspill illustrated in Fig. 5, it can be seen that, for the field steering lead, it tends to be lower and more spread over the bins of the histogram.

The scores obtained from this analysis are summarized in Table II. There is a significant decrease in the number of cases with the activated volume covering the whole target area for the field steering lead and the mean is slightly lower

TABLE II

STATISTICAL RESULTS FOR ALL OF THE LEADS

	Conventional	Field steering
Stimuli with ≥90% activation	47%	30%
Activation mean	73.6%	63.4%
Overspill mean	81.3%	71.6%
Overspill standard deviation	10.2%	18.1%

as well. On the other hand, there is a reduction of about 12.0% in the overspill mean value for the field steering lead compared to the conventional one. This comes however with an increase in the standard deviation.

IV. DISCUSSION

Using excessive stimuli amplitude in DBS is known to cause side effects. According to [10], [11], field steering leads can be potentially used for tailoring the activated volume to the target area while restricting the electric field spread beyond by means of asymmetrical stimulation. This study provides a quantitative analysis of the extent to which an asymmetrical configuration could achieve this end.

First, for a single patient, the field asymmetry is shown to result in a decrease of 22% in the overspilled volume, while preserving the same activation of the target area. Although this number might not seem impressive, it must be taken into account that, for the symmetrical stimuli, most of the stimulated volume lay outside of the target area. Therefore the decrease achieved by the field steering lead might have a significant impact regarding possible side effects.

Further, a sizable sample of 82 leads was analyzed to compare the performance of both kinds of leads. A mean value decrease of 12.0% was observed in the overspill at the expense of a larger standard deviation. However, it should be noted that in some cases there is no coverage with the provided settings, as shown in Fig. 4. In addition, in some cases similar activation is achieved, but in most of them both reduced activation and overspill are obtained, which implies a trade-off relation between target selectivity and activation. Still, the decrease in the overspilled activated volume is significant in general and it might improve therapeutic results. To quantify its effects in detail, further research should relate those volumes with real therapeutic data.

The model used in the present study has some limitations. First, the brain tissue was assumed to be homogeneous, when this is not the case and significant (patient specific) differences may arise (see [8]). Furthermore, the encapsulation layer surrounding the lead has uncertain properties, such as the conductivity and the thickness. Worse yet, it might be time varying, as was observed in [12]. In addition, the selected field threshold is also valid for a certain kind of neuron, a certain pulse width, and a certain kind of stimuli. Since the stimulated area may be populated by several kinds of neurons, it should be taken into account when selecting the threshold. Thus, a more thorough analysis would have to deal with time-dependent stimuli of neuron populations and is beyond the scope of this paper.

Despite the mentioned limitations, this study highlights the difference between the two considered leads and demonstrates how, given real stimulation settings and lead positions, stimulating with a lead capable of asymmetrical stimulation might yield less overspill of the potential target.

ACKNOWLEDGMENTS

The authors would like to thank Luc Mallet's group, the Pitié-Salpêtrière University Hospital, Paris and Sapiens Steering Brain Stimulation BV for kindly providing the clinical data used in this study.

REFERENCES

[1] J. A. Obeso and R. Olanow, C. W., Rodriguez-Oroz, M. C., Krack, P., Kumar, Deep-Brain Stimulation of the Subthalamic Nucleus or the Pars Interna of the Globus Pallidus in Parkinson's Disease, N. Engl. J. Med., vol. 345, no. 13, pp. 956-963, 2001.

[2] N. Suthana, Z. Haneef, J. Stern, R. Mukamel, E. Behnke, B. Knowlton, and I. Fried, Memory enhancement and deep-brain stimulation of the entorhinal area, N. Engl. J. Med., vol. 366, pp. 502-510, 2012.

[3] I. Isaias, R. Alterman, and M. Tagliati, Deep brain stimulation for primary generalized dystonia: Long-term outcomes, Arch. Neurol., vol. 66, no. 4, pp. 465-470, 2009.

[4] L. Gabriels, P. Cosyns, B. Meyerson, S. Andreewitch, S. Sunaert, A. Maes, P. Dupont, J. Gybels, F. Gielen, and H. Demeulemeester, Long-term electrical capsular stimulation in patients with obsessivecompulsive disorder, Neurosurgery, vol. 52, pp. 1263-1274, 2003.

[5] J. Kuhn, M. Bodatsch, V. Sturm, D. Lenartz, J. Klosterkotter, P. Uhlhaas, C. Winter, and T. Grundler, Deep Brain Stimulation in Schizophrenia, Fortschritte der Neurol. Psychiatr., vol. 79, pp. 632-641, 2011.

[6] R. Gross and A. Lozano, Advances in neurostimulation for movement disorders, Neurol Res., vol. 22, pp. 247-258, 2000.

[7] P. F. D' Haese, S. Pallavaram, P. E. Konrad, J. Neimat, J. M. Fitzpatrick, and B. M. Dawant, Clinical accuracy of a customized stereotactic platform for deep brain stimulation after accounting for brain shift, Stereotact. Funct. Neurosurg., vol. 88, no. 2, pp. 81-87, Jan. 2010.

[8] A. Chaturvedi, C. R. Butson, S. F. Lempka, S. E. Cooper, and C. C. McIntyre, Patient-specific models of deep brain stimulation: influence of field model complexity on neural activation predictions., Brain Stimul., vol. 3, no. 2, pp. 65-67, Apr. 2010.

[9] P. Krack, A. Mendes, A. Benabid, and P. Pollak, Postoperative Management of Subthalamic Nucleus Stimulation for Parkinson's Disease, Mov. Disord., vol. 17, Suppl. 3, pp. 188-197, 2002.

[10] J. Buhlmann, L. Hofmann, P. a Tass, and C. Hauptmann, Modeling of a segmented electrode for desynchronizing deep brain stimulation., Front. Neuroeng., vol. 4, no. December, p. 15, Jan. 2011.

[11] E. Toader, M. M. J. Decré, H. C. F. Martens, and A. T. Dbs-array, Steering deep brain stimulation fields using a high resolution electrode array, in 32nd Annual International Conference of the IEEE EMBS, 2010, pp. 2061-2064.

[12] W. M. Grill and J. T. Mortimer, Electrical properties of implant encapsulation tissue., Ann. Biomed. Eng., vol. 22, no. 1, pp. 23-33, 1994.

[13] D. Andreuccetti, R. Fossi, and C. Petrucci, Dielectric properties of body tissue, 2005. Available: http://niremf.ifac.cnr.it/tissprop/.

[14] X. Vasques, L. Cif, G. Mennessier, and P. Coubes, A Target-Specific Electrode and Lead Design for Internal Globus Pallidus Deep Brain Stimulation, Stereotact. Funct. Neurosurg., vol. 88, pp. 129-137, 2010.

[15] R. Cubo, M. Åström, and A. Medvedev, Stimulation field coverage and target structure selectivity in field steering brain stimulation, Mov. Disord., vol. 29, no. S1, pp. S198-S199, 2014.

[16] M. Åström, L. U. Zrinzo, S. Tisch, E. Tripoliti, M. I. Hariz, and K. Wårdell, Method for patient-specific finite element modeling and simulation of deep brain stimulation., Med. Biol. Eng. Comput., vol. 47, no. 1, pp. 21-28, Jan. 2009.

[17] D. R. McNeal, Analysis of a model for excitation of myelinated nerve, IEEE Trans. Biomed. Eng., vol. 23, no. 4, pp. 329-337, Jul. 1976.

[18] F. Rattay, Analysis of models for external stimulation of axons, IEEE Trans. Biomed. Eng., vol. 33, pp. 974-977, 1986.